COMMISSIONING OF ELECTRON BEAM COOLING AT S-LSR*

T. Shirai[#], S. Fujimoto, M. Ikegami, A. Noda, H. Tongu, M. Tanabe, H. Souda
ICR, Kyoto-U, Uji, Kyoto, Japan,
K. Noda, NIRS, Anagawa, Inage, Chiba, Japan,
T. Fujimoto, H. Fujiwara, S. Iwata, A. Takubo, T. Takeuchi, S. Shibuya
AEC, Anagawa, Inage, Chiba, Japan,
E. Syresin, I. Seleznev, A. Smirnov, I. Meshkov, JINR, Dubna, Moscow Region, Russia
H. Fadil, MPI Kernphysik, Spaupfercheckweg, Heidelberg, Germany

Abstract

The electron cooler at S-LSR was designed to maximize the effective cooling length in the limited space. The magnetic field of the cooler was calculated precisely by the 3-D program code and the effective cooling length became 0.44 m while the total length of the cooler is 1.8 m. The electrostatic deflectors are used in the troid to decrease the electron beam loss rate, which is 2×10^{-4} now.

The commissioning of the electron cooling was started from November 2005. In the first day, the cooling of 7MeV proton beam was observed. The maximum cooling force is 0.12 eV/m with the electron current of 56 mA. The attainable lowest momentum spread of protons is 5×10^{-6} at 10^4 protons.

Two kinds of the ion beam instabilities were observed. The vertical coherent instability was succeeded to be damped by the feedback and the stored current of 1.2mA was achieved. The maximum current is limited by the initial loss now.

INTRODUCTION

S-LSR is a new ion cooler in Kyoto University, which has an electron cooler and a laser cooling system. The electron cooling will be used for the cooling of the laser accelerated ions and the short pulse beam generation using the electron cooling and the RF phase rotation [1, 2]. Figure 1 shows the cross-sectional view of the electron
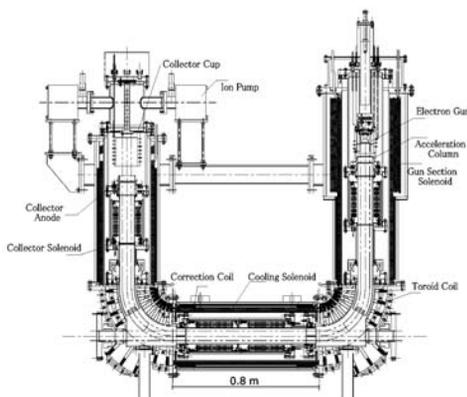
Table 1 Main parameters of S-LSR and cooler.

Ring	
Circumference	22.557 m
Length of Drift Space	1.86 m
Number of Periods	6
Average Vacuum Pressure	10 nPa (typ.)
Electron Cooler (for 7MeV p$^+$)	
Energy	3.842 keV
Electron Beam Current	107 mA (typ.)
Beam Diameter	50 mm
Beam Density	9.2×10^6 e$^-$/cm^3
Solenoid Field in the central	500 Gauss
Expansion Factor	3
Cooler Solenoid Length	800 mm
Effective Cooling Length	440 mm

cooler and table 1 shows the main parameters of S-LSR and the cooler parameters for 7 MeV proton.

The commissioning of the electron cooling was started from November 2005, following the beam commissioning of S-LSR in October 2005. The injected beam was 7 MeV protons from the existing RF linac.

ELECTRON COOLER

The design issue of the electron cooler was to develop a compact one to install the short drift space (1.86 m) [3]. On the other hand, the high cooling force is necessary for the fast cooling. The following designs were adopted.

1. A high perveance electron gun is used and the hollow beam generation is also considered.
2. An electrostatic deflector is installed in the troid to compensate the drift motion of the electron beam [4]. It is effective to reduce the beam loss even though the electron beam aperture is small.
3. 6 vertical correction coils are installed to extend the effective cooling length in the central solenoid. The effective length is 440 mm where the magnetic field homogeneity is +/-2x10^{-4}, while the cooling solenoid length is 800 mm.

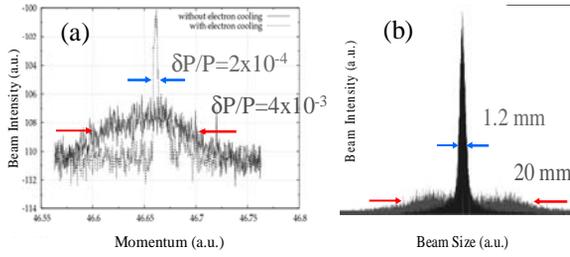Figure 1 View of the electron cooler at S-LSR.

Figure 2 Momentum spread (a) and the horizontal profile (b) of 7MeV proton beam before and after the electron cooling. They are measured by Schottky monitor and the residual gas monitor using MCP, respectively.
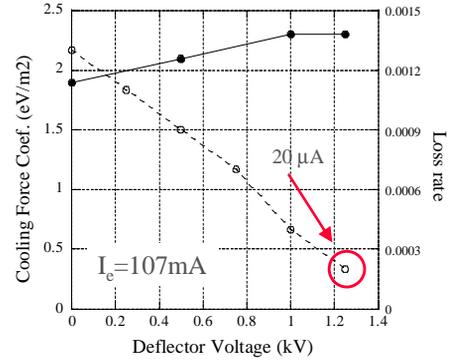

Figure 3 Cooling force and the electron loss rate with various deflector voltages with the current of 107mA
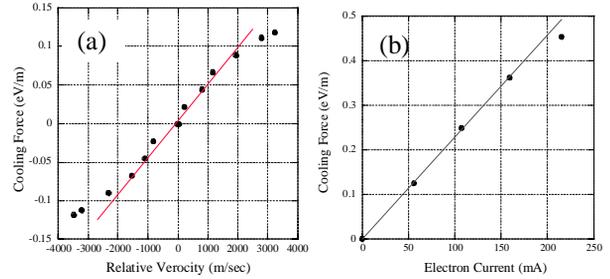

Figure 4 (a) Cooling force with the electron current of 56 mA (4.8×10^6 e$^-$/cm^3) as a function of the relative velocity. (b) The electron current dependence of the maximum cooling force.

4. Horizontal ion steering magnets are installed in the troid section to save the space and to minimize the closed orbit distortion of ion beams.

Figure 2 shows the typical longitudinal and transverse beam profile before and after the cooling. They are measured by the Schottky monitor and the residual gas monitor using MCP, respectively. When the ion beam current is 30 μA and the electron current is 107 mA, the momentum spread and the horizontal beam size become 2×10^{-4} and 1.2 mm, respectively [5].

We measured the electron loss current and the cooling force with various deflector voltages in the troid to confirm the effect of the above design item 2. The results are shown in Fig.3. When the deflector voltage was changed, the compensation magnetic field in the troid was also changed to keep the electron orbit constant. When the voltage was 1.25 kV, there was no magnetic field for the compensation. The loss rate becomes 1/6, while the cooling force is almost independent on the voltage. The vacuum pressure was also improved due to the small loss, which was 4×10^{-9} Pa with the electron beam of 107 mA. The small change of the cooling force was induced by the shift of the vertical closed orbit distortion.

In order to optimize the electron cooling, the electron and the ion axis must be aligned to be parallel by the steering coils. The allowable error of the alignment angle not to reduce the cooling force was 2×10^{-4} rad, which is consistent with the magnetic field homogeneity in the cooling section. Fig.4 (a) shows the cooling force normalized by the cooler length with the electron current of 56 mA ($=4.8 \times 10^6$ e$^-$/cm^3) which was measured using the induction accelerator. It shows the cooling force at the small relative velocity region. The slope in the linear region is 4.8×10^{-5} eVs/m^2 and it has a maximum value of 0.12 eV/m at the relative velocity of +/-3500 m/sec.

Fig.4 (b) shows the electron current dependence of the maximum cooling force. The cooling force is proportional to the electron current except 215 mA. It is supposed that the space charge of the electron beam induces the heating above 215 mA.

The electron temperature is an important parameter for the electron cooler. It is given by [6],

where T_{cath} is a cathode temperature of 900 °C for S-LSR cooler and α is an expansion factor of 3. When the electron current is 50 mA, the longitudinal temperature is 50 μeV and the transverse one is 34 meV. The longitudinal temperature of the electron beam is very low due to the static acceleration but it is easily affected by external heating such as ripples of the power supplies for the electron beam and the ring magnets. The inhomogeneous magnetic field in the cooling section is also a heating source.

The straightforward way to check the longitudinal electron temperature is a measurement of the lowest temperature of the ion beam because it is equal to the electron temperature. Figure 5 shows the measured ion momentum spread as a function of the ion particle number with the electron current of 50 mA. The lowest momentum spread is 5×10^{-6}, which corresponds to the 300 μeV from the following relation,

$$k_B T_{e//} = \frac{(k_B T_{cath})^2}{2eU} + C \frac{e^2 n_e^{1/3}}{4\pi\varepsilon_0} \qquad (1)$$

$$k_B T_{e\perp} = \frac{k_B T_{cath}}{\alpha}$$

$$k_B T_{i//} = m_i v_0^2 \left(\frac{\delta p}{p}\right)^2. \qquad (2)$$
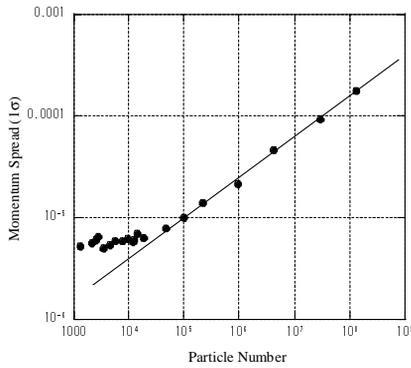
D. Beam cooling and intra-beam scattering

Figure 5 Momentum spread of the ion beam as a function of the ion particle number with the electron current of 50 mA.

It is higher than the expected value and the improvements of the cooler system are still necessary.

BEAM INSTABILITY

Figure 6 (a) shows the stored current measured by the DC current transformer. The proton beam is injected every 20 sec with the electron current of 107 mA. Two kinds of instability are found. One is an initial beam loss. Most of the new injected beam is lost after the injection with the decay time of 10 - 20 seconds. The similar loss of proton is reported in COSY [7]. It seems that it is a slow phenomenon without a coherent oscillation.

The other is a coherent loss (see Fig.6 (a)). When the ion current exceeds 400 μA, the large beam loss is sometimes observed even for the coasting beam. At the
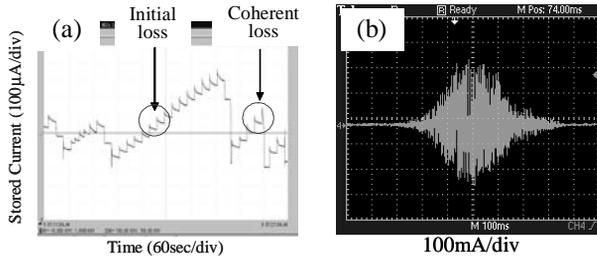

Figure 6 (a) DC current transformer signal during the cooled beam stacking. (b) Difference signal between the upper and lower electrostatic plates when the coherent loss occurs.
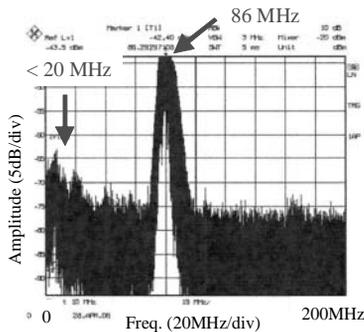

Figure 7 Frequency spectrum of signal of the electrostatic pickup at the ion current of 450 μA.

same time, the vertical coherent oscillation is also observed. Figure 6 (b) is a differential signal between the upper and lower electrostatic plates. The growth rate is about 100 msec. This vertical growth of the betatron amplitude leads to the beam loss because the vertical aperture is smaller than the horizontal one.

Figure 7 is a frequency spectrum of the electrostatic pickup signal at the ion current of 450μA. Below 20 MHz, some harmonics of the vertical betatron sidebands are always excited but the amplitude is small and they do not lead to the beam loss. Sometimes strong peak of the harmonics of the vertical betatron sidebands appears around 86 MHz. After the growth of the coherent oscillation, the oscillation frequency is gradually changed from 86 MHz and then it damps. It is correlated to the beam loss in Fig.6 (a) and the vertical coherent oscillation in Fig.6 (b).

We tested a vertical feedback damping system. It consists of pickups, RF filters, attenuators, delays and an RF amplifier. After the timing adjustment, we succeeded to suppress the vertical coherent oscillation and the beam loss. The final ion current was 1.2 mA, which was limited by the initial loss.

We found two features in the feedback experiments. One is a very critical synchronous timing between the ion beam and the feedback signal. The allowable error is 2 nsec. It is supposed that it is originated from the high frequency component of the vertical coherent oscillation. The other feature is a growth of the horizontal coherent oscillation. The frequency components are below 20 MHz. They are excited stationary but it does not induce the beam loss because the oscillation amplitude is still small at the ion current of 1.2 mA and the horizontal aperture is large.

ACKNOWLEDGMENTS

REFERENCES

[1] A. Noda et al., Proc. of Symposium on Accel. Sci. and Tech. (2001) 125.

[2] T. Fujimoto et al., Beam Science and Technology, 10, (2006).

[3] Fadil H Grieser M Noda A Noda K Shirai T and Syresin E, Nuclear Instruments and Methods, Vol. 532, Issues 1-2, 11 (2004) 446-450

[4] V. Bocharov et al., Nuclear Instruments and Methods in Physics Research Section A, Vol. 532, Issues 1-2, 11 (2004) 144-149

[5] H. Fadil et al., HIMAC Report-111 (2006).

[6] Kudelainen V.I Lebedev V.A Meshkov I.N Parkomchuk V.V and Sukhina B.N 1982 *Soy. Phys. JETP* **56** 1191.

[7] J. Dietrich, Proceedings of this Workshop.